



OPEN

Neuroprotective effects of L-Dopa-modified zinc oxide nanoparticles on the rat model of 6-OHDA-induced Parkinson's disease

Yesim Yeni¹✉, Sıdıka Genc², Muhammed Sait Ertugrul³, Hayrunnisa Nadaroglu⁴, Arzu Gezer⁵, Ali Sefa Mendil⁶ & Ahmet Hacimuftuoglu⁷

Parkinson's disease (PD) is a chronic neurodegenerative case. As the disease progresses, the response time to doses of levodopa (L-Dopa) becomes shorter and the effects of the drug are severely limited by some undesirable side effects such as the 'on-off' phenomenon. In several diseases, including Parkinson's, nanoparticles can deliver antioxidant compounds that reduce oxidative stress. This study evaluates and compares the neuroprotective effects of L-Dopa-modified zinc nanoparticles (ZnNPs) in the 6-hydroxydopamine (6-OHDA)-induced PD rat model. For this purpose, the synthesis of NPs was carried out. Scanning electron microscopy, X-ray diffraction and Fourier transform infrared spectrophotometer were used for characterization. The rats were randomized into 9 experimental groups: control, lesion group (6-OHDA), 6-OHDA + 5 mg/kg L-Dopa, 6-OHDA + 10 mg/kg L-Dopa, 6-OHDA + 20 mg/kg L-Dopa, 6-OHDA + 20 mg/kg ZnNPs, 6-OHDA + 40 mg/kg ZnNPs, 6-OHDA + 30 mg/kg ZnNPs + L-Dopa, and 6-OHDA + 60 mg/kg ZnNPs + L-Dopa. Behavioral tests were performed on all groups 14 days after treatment. Phosphatase and tensin homolog, Excitatory amino acid transporter 1/2, and Glutamine synthetase gene analyses were performed on brain samples taken immediately after the tests. In addition, histological and immunohistochemical methods were used to determine the general structure and properties of the tissues. We obtained important findings that L-Dopa-modified ZnNPs increased the activity of glutamate transporters. Our experiment showed that glutamate increases neuronal cell vitality and improves behavioral performance. Therefore, L-Dopa-modified ZnNPs can be used to prevent neurotoxicity. According to what we found, results show that L-Dopa-modified ZnNPs will lead to the effective avoidance and therapy of PD.

Keywords 6-OHDA, EAAT 1/2, GLUL, L-Dopa, PTEN, ZnNP

Parkinson's disease (PD) is an advancing, chronic neurodegenerative illness defined as tremor paralysis that requires ongoing treatment. The illness is characterized by the degeneration of dopaminergic neurons in the substantia nigra, causing a reduction in dopamine in the striatum^{1,2}. Clinically, the disease is related to many motor symptoms like bradykinesia, dementia, rigidity, and tremor, as well as several non-motor symptoms like depression^{3,4}. Current treatments for PD focus on lightening motor symptoms by making up for dopamine lack. Among the treatments, levodopa (L-Dopa) is the gold standard, and its use provides significant healing in patients' quality of life for a limited period⁵. Unluckily, as the illness progresses, fewer residual nigrostriatal neurons can take up exogenously applied L-Dopa and convert it to dopamine for subsequent storage and release⁶.

¹Department of Medical Pharmacology, Faculty of Medicine, Malatya Turgut Ozal University, 44210 Battalgazi, Malatya, Turkey. ²Department of Medical Pharmacology, Faculty of Medicine, Bilecik Şeyh Edebali University, Bilecik, Turkey. ³Department of Food, Feed and Medicine, Hemp Research Institute, Ondokuz Mayıs University, Samsun, Turkey. ⁴Department of Food Technology, Vocational College of Technical Science, Ataturk University, 25240 Erzurum, Turkey. ⁵Department of Health Care Services, Vocational School of Health Services, Ataturk University, 25240 Erzurum, Turkey. ⁶Department of Pathology, Faculty of Veterinary Medicine, Erciyes University, Kayseri, Turkey. ⁷Department of Medical Pharmacology, Faculty of Medicine, Ataturk University, Erzurum, Turkey. ✉email: yesim.yeni@ozal.edu.tr

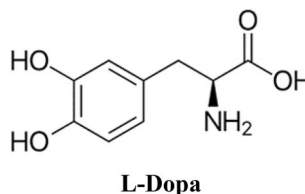
As a result, as PD progresses, the response time to individual dosages of L-Dopa becomes shorter in the majority of patients and the drug's effects are severely limited by some undesirable side effects, such as the 'on-off' phenomenon^{7,8}. In addition, L-Dopa metabolism produces various free radicals that cause the loss of nigrostriatal dopaminergic neurons and the development of the disease^{9,10}.

The blood–brain barrier restricts the reach of therapeutic molecules and macromolecules¹¹. Therefore, a major therapeutic challenge in the therapy of PD is to develop an effective drug-targeting system that can improve symptoms, prolong the delivery of L-Dopa to the brain across the blood–brain barrier, prevent fluctuations in its concentration, and reduce the ratio of neurodegeneration. It can deliver antioxidant compounds that decrease oxidative stress in diverse diseases, including PD, which is critical for nanoparticles to exert a therapeutical effect^{12,13}. With advances in medicine, recent nanotechnology-based approaches have been used in medicine delivery systems that can cross the blood–brain barrier¹⁴. Molecules and the associated medicine can be attached to these delivery systems, which can then be actively transported and targeted to specific injured tissues or organs. The basic purpose of using nano-sized medicine delivery systems in PD is to raise drug availability in the brain without increasing the dosage, thereby decreasing medicine side effects¹⁵. Therapy of cancer and various other diseases with nanoparticles or gold shields are some of the most significant applications in this area. Nanotechnology also offers novel occasions in implantable drug delivery systems, which are often preferred to injectable drugs¹⁶. This study aims to evaluate and compare the neuroprotective effects of L-Dopa-modified zinc nanoparticles (ZnNPs) on the 6-OHDA-induced PD rat model.

Materials and method

Preparation and characterization of L-Dopa modified ZnNPs

Zinc chloride (ZnCl_2), urea ($(\text{NH}_2)_2\text{CO}$), trisodium citrate dihydrate ($\text{C}_6\text{H}_5\text{Na}_3\text{O}_7$, 98%), L-Dopa ($\text{C}_9\text{H}_{11}\text{NO}_4$), methanol ($\text{CH}_3\text{-OH}$) and whole other chemicals were bought from Sigma-Aldrich. For the synthesis of ZnNPs, ZnCl_2 (0.1 M) stock solutions were prepared by stirring in 50 ml distilled water. Then 0.2 g $(\text{NH}_2)_2\text{CO}$ and 0.65 g $\text{C}_6\text{H}_5\text{Na}_3\text{O}_7$ were suffixed to the solution and mixed in a magnetic mix for 30 min. To this solution, 0.5 M 25 ml NaOH solution was suffixed with constant mixing up to the pH of the reaction medium between 8 and 11. The solutions were then transferred to Teflon-lined, sealed stainless steel autoclaves and held at 180–200 °C under autogenous pressure for 8 h. They were then left to cool naturally to room temperature. At the end of the reaction, the resulting white solid ZnNPs were washed with methanol, filtered, and then dried under vacuum in a laboratory oven at 60 °C¹⁷.



The L-Dopa solution, prepared at a dose of 2 mg/ml⁻¹, was suffixed to the ZnNPs and, after thorough dispersion, stirred at room temperature for half an hour to ensure binding between the $-\text{NH}_2$ and $-\text{COOH}$ groups. The ZnNPs were then gathered by centrifugation at 3500×g for 5 min and the ZnNPs were washed to remove unbound L-Dopa and stored at +4 °C up to use. The preparation of L-Dopa-modified ZnNPs was achieved by physically adsorbing L-Dopa onto ZnNPs instead of chemical bonds.

The characterization of the NPs was carried out at Atatürk University, Eastern Anatolia High Technology Application and Research Center. The equipment used for characterization is listed below: Scanning Electron Microscope (SEM) for SEM analysis: Zeiss brand Sigma 300 model, X-ray diffraction (XRD): Panalytical brand Empyrean model, Fourier transform infrared spectrophotometer (FTIR): Bruker model Vertex 70 was used.

Animals and experimental procedure

The present study was conducted in compliance with the ARRIVE guidelines. A total of 72 male Sprague–Dawley rats weighing 250–300 g were used in this study and were obtained from the Atatürk University Medical Experimental Research and Application Centre. The animals were given adequate amounts of water and food throughout the study. All animals included in the test were separated into groups and housed in cages in the laboratory environment with a room temperature of 22 ± 1 °C and a 12-h day–night cycle. It was approved by the "Atatürk University Animal Experiments Local Ethics Committee" with a letter dated 03.08.2023 and number E-42190979-000-2300239671 that all stages of our study comply with ethical rules.

Rats were randomly divided into 9 experimental groups: (1) sham-operated (control, n = 8), (2) lesion group (6-OHDA, n = 8) at a dose of 8 µg/µl, (3) lesion group treated with 5 mg/kg L-Dopa (Sigma-Aldrich, USA) (6-OHDA + L-Dopa, n = 8), (4) lesion group treated with 10 mg/kg L-dopa (6-OHDA + L-Dopa, n = 8), (5) lesion group treated with 20 mg/kg L-dopa (6-OHDA + L-Dopa, n = 8), (6) Lesion group treated with 20 mg/kg ZnNP (6-OHDA + ZnNP, n = 8), (7) Lesion group treated with 40 mg/kg ZnNP (6-OHDA + ZnNP, n = 8), (8) Lesion group treated with 30 mg/kg ZnNP + L-Dopa (6-OHDA + ZnNP (20 mg/kg) + L-Dopa (10 mg/kg), n = 8) and (9) Lesion group treated with 60 mg/kg ZnNP + L-Dopa (6-OHDA + ZnNP (40 mg/kg) + L-Dopa (20 mg/kg), n = 8). Doses were selected based on previous studies^{18–20}. To increase the effect of 6-OHDA on dopamine neurons and prevent damage to noradrenergic neurons, desipramine hydrochloride (single dose 30 mg/kg i.p.) and pargyline hydrochloride (single dose 10 mg/kg i.p., Sigma-Aldrich, USA) were administered before application.

Anesthetized (75 mg/kg ketamine (Ketalar 500 mg injectable 1 vial, Pfizer, Turkey) and 8 mg/kg xylazine (Xylazole 20 ml injectable 1 vial, Provet, Turkey) rats were located in the stereotaxic apparatus and their heads were fixed. To set up the experimental model of PD, the coordinates of the area to be injected were determined unilaterally in the right hemisphere according to the rat brain atlas as anteroposterior – 5.5 mm (from the bregma), lateral 2 mm (from the midsagittal suture) and dorsoventral 8 mm (from the cranial surface)²¹. Then, a total amount of 8 µg/µl of 6-OHDA (Sigma-Aldrich, USA) was dissolved in 0.1% ascorbic acid (Sigma-Aldrich, USA) physiological saline solution and injected unilaterally into the substantia nigra region of the rats using a Hamilton syringe in a volume of 4 µl using the stereotaxic method. At the same time, the same coordinates were entered in the same way and the rats in the control group were given saline. After all procedures were completed, the animals' cranial skins were cleaned with povidone-iodine and sutured. Starting the next day, animals in the control and 6-OHDA groups were given saline intraperitoneally for 14 days, while the treatment groups (6-OHDA + L-Dopa, 6-OHDA + ZnNP, 6-OHDA + ZnNP + L-Dopa) were given drugs by gavage for 14 days. After 14 days, behavioral tests were performed in all groups. PTEN, EAAT 1/2, and GLUL gene analyses were performed on brain samples taken immediately after the tests. In addition, histological and immunohistochemical methods were used to determine the general structure and properties of the tissues.

Apomorphine rotational test

The apomorphine-induced rotation test is a commonly used method to demonstrate the effect of lesions on the dopaminergic system and the efficacy of treatment in rats created to model PD²². Rats that rotated continuously in the same direction 7 times per minute in the apomorphine-induced rotation test were considered to have PD²³. At the end of drug and saline administration, the apomorphine-induced rotation test was repeated. Briefly, mice were let to adapt for 5 min and complete turns were counted after intraperitoneal injection of the drug apomorphine hydrochloride (Sigma-Aldrich, USA; 2.5 mg/kg) in a cylindrical container (diameter = 28 cm, height = 38 cm). After injection, the animals were video-recorded for 30-min. These 30 min recordings were then reviewed and the number of 360-degree (contralateral) rotations observed in the animals was calculated. Rats with more than 7 rotations were used as valid pathology models.

Locomotor activity test

Plexiglas cages (O'Hara and Co., Ltd., Tokyo, Japan) measuring 42 × 42 × 42 cm were used to measure the locomotor activity of the experimental animals. This system was used to measure the resting time and the sum distance traveled by the rats during the experiment. For all parameters studied, the rats were located individually in the center of the Plexiglas cages and recorded for 20 min. This test was used to detect increases or decreases in the locomotor activity of the rats.

Elevated plus maze test

Anxiety-like behavior was evaluated using the elevated plus maze (50 × 14 × 50 cm; O'Hara and Co., Ltd., Tokyo, Japan). Every rat was located in the central field of the labyrinth facing one of the open arms. Duration spent in the open arms was evaluated over 5 min using the EthoVision XT video imaging system²⁴.

Cylinder test

The cylinder test is based on measuring and scoring the use of each front paw during spontaneous exploration in animals. It is used to assess motor asymmetry and Parkinsonian motor symptoms^{25,26}.

Rats were located in a sheer Plexiglas cylinder 20 cm in diameter and 40 cm in height. Each animal was recorded for 60 min and scored individually. Situations in which the animals used both their right and left front paws to touch the cylinder wall and those in which they used their right and left paws separately to touch the cylinder wall were monitored and compared with the total number of paw uses. The results were expressed as percentages and the calculation was made as follows: the sum of the total number of times the right foot, left foot and both feet touched the cylinder wall is 100%, from which the percentage for each finding was calculated.

Real-time PCR

Homogenized brain tissue samples were insulated using the High Pure RNA Isolation Kit (Cat. No. 11828665001). RNA samples for cDNA were readied using the Transcriptor First Strand cDNA Synthesis kit (Cat. No. 04896866001) (Roche, Basel, Switzerland) to the specified protocol.

Real-time PCR was made using primers designed for rat β-actin Rn00667869_m, Slc1a3 Rn01402419_m1, PTEN mRatBN7.2:CM026974, Glul Rn01483107_m1, and Slc1a2 Rn01275814_m1. Values were computed by calculating $2^{-\Delta\Delta C_t}$ from Real-Time PCR CT data²⁷.

Histopathological method

Rats were necropsied and brain tissue was fixed in 10% neutral formalin. Tissues were subjected to routine alcohol-xylene processing and buried in paraffin blocks. 5 µ sections were cut on poly-lysine slides, stained with hematoxylin–eosin. Pyknotic changes in neurons and glial cell activation in the substantia nigra region of each sample were evaluated across five different microscope fields according to Table 1.

Immunohistokimyasal method

Rats were necropsied and brain tissue was fixed in 10% neutral formalin. Tissues were subjected to routine alcohol-xylene processing and buried in paraffin blocks. 5 µ sections taken on polylysine slides were undergone through a series of xylol and alcohol, washed with PBS, and incubated in 3% H₂O₂ for 10 min to inactivate

Pyknotic neurons among all neurons	Glial cell count
5% < (-), absent	15 < Normal
6–40% (+), mild	16–30 glial cells (+), mild
41–70% (++) , moderate	31–45 glial cells (++) , moderate
>71% (+++) , severe	>46 glial cells (+++) , severe

Table 1. Histopathological scoring.

endogenous peroxidase. To disclose the antigen in the tissues, they were treated with antigen retrieval solution for 2×5 min at 500 watts. The tissues were then washed with PBS and incubated with primary antibodies against alpha-synuclein (Santa Cruz, Cat. No. sc-69977 1/400 dilution) and GFAP (Abcam, Cat. No. ab7260 1/400 dilution) at room temperature for 45 min. Secondary; large volume detection system: anti-polyvalent, HRP (ThermoFischer, catalogue no. TP-125-HL) was used as recommended by the manufacturer. 3,3'-diaminobenzidine was used as chromogen. After counterstaining with Mayer's hematoxylin, sections were coverslipped with Entellan and examined by light microscopy. The percentage areas of immunopositivity in the substantia nigra region of each sample were evaluated across five different microscope fields in the Image J program according to Table 2.

Statistical analysis

Tukey's least important distinction test was used after a one-way ANOVA to assess the results acquired in the behavioral alterations that emerge with stress. Statistical analyses were also performed using 'SPSS 22.0' (IBM, Armonk, NY, USA), and results less than or equal to $p < 0.05$ were considered statistically important. Histopathological and immunohistochemical data were analyzed using SPSS 20.00 software. The distinction between groups was specified by the non-parametric Kruskal–Wallis test and the distinction between groups was specified by the Mann–Whitney U test ($p < 0.05$).

Results

UV analysis

Figure 1 shows the absorption spectra in the 200–800 nm range obtained by monitoring the reaction environment of ZnNPs. In the green hydrothermal synthesis of ZnNPs, the absorption was scanned in the range of 300–400 nm and it was found that it gave a broad peak in the interval of 200–400 nm. The synthesis of ZnNPs was realized at 180 °C for 6 h and the absorbance was measured at a maximum of 368 nm in the samples taken from the reaction medium.

α -Synuclein	GFAP
5 < (-), absent	5 < (-), absent
6–20% < (+), mild	6–30 < (+), mild
21–30% (++) , moderate	31–60 (++) , moderate
>31% (+++) , severe	>61 (+++) , severe

Table 2. Percentage of immunopositive area in the field.

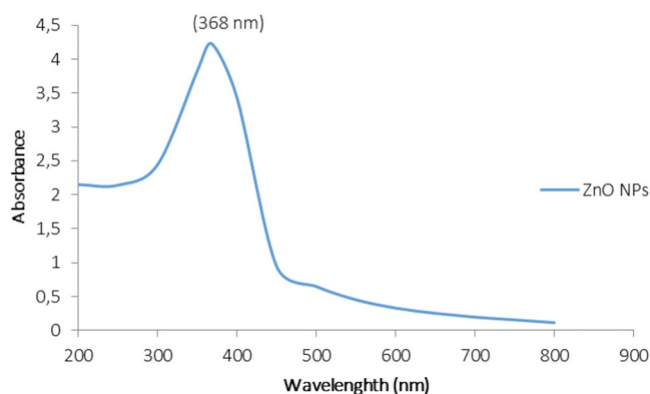


Figure 1. UV spectra of ZnNPs: ZnNPs wavelength scan.

XRD analysis

Figure 2 shows the XRD patterns of the synthesized ZnNPs. X-ray diffraction data were registered using Cu K α radiation (1.5406 Angstroms). Density data were gathered over a 2θ interval of 20° – 80° . The mean grain size of the samples was calculated from the diffraction intensity of the (101) peak using the Scherrer equation. X-ray diffraction studies showed that the synthesized materials were wurtzite phase ZnO and the diffraction peaks agreed with the reported JCPDS data; no characteristic peaks were observed except for ZnO. The grain size (D) of the particles was specified from the XRD line widening measurement using the average. Scherrer equation:

$$D = \frac{0.89\lambda}{\beta \cos\theta}$$

A clear line widening of the diffraction peaks indicates that the synthesized materials are in the nanometre interval. A clear line widening of the diffraction peaks indicates that the synthesized ZnNPs are in the nanometer interval. The calculated cage parameters are also in compliance with the reported rates. The reaction temperature has a strong influence on the particle morphology of the prepared ZnO powders. The average crystal size of the zinc nanoparticles was determined to be 21.3 nm using Scherrer's formula. The results obtained are compatible with the literature and are similar to the XRD patterns of ZnNPs obtained by Arefi and Rezaei-Zarchi using green synthesis²⁸.

FTIR spectrometer

ZnNPs obtained by green synthesis were analyzed with the FTIR spectroscopy technique. The band of 1500 – 600 cm^{-1} showed the fingerprint area of ZnNPs. The powerful peak was observed at the frequency of 1627 cm^{-1} , indicating N–H twisting, and poor peaks were found at 1450 cm^{-1} and 1641 cm^{-1} (Fig. 3), which are attributed to the symmetric and asymmetric vibration of C=O²⁹. The wide peak at 3456 cm^{-1} indicates the –OH tension link vibration resulting from water adsorption on the surface of ZnO NPs, while the peak at 468.7 cm^{-1} was attributed to the Zn–O tension vibration.

SEM of ZnNPs

SEM analysis was realized to specify the surface morphology of the ZnNPs obtained by green synthesis. As can be viewed from the images, the synthesized ZnNPs are in good deal with the result obtained by XRD analysis.

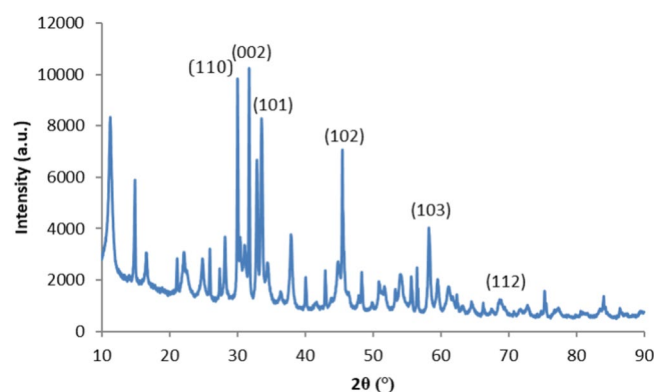


Figure 2. XRD patterns of ZnNPs.

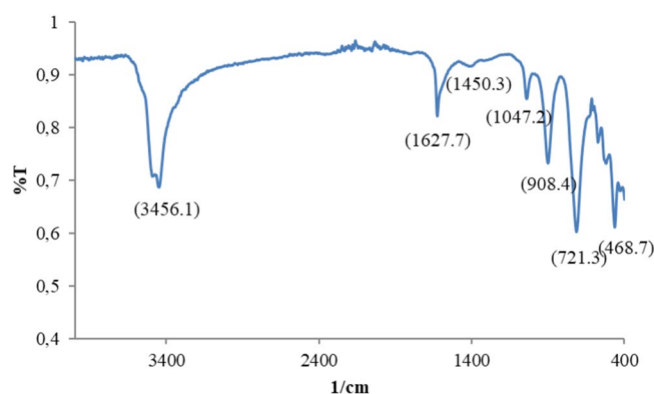


Figure 3. FTIR spectrum of ZnNPs.

In Fig. 4, it is seen that accumulation has occurred and that there is agglomeration between ZnNPs, although not too much. In addition, the synthesized ZnNPs have a spherical shape. The results obtained are compatible with the literature^{30–32}.

Effects of L-Dopa modified ZnNPs on 6-OHDA-induced motor disorders

The effect of lesions resulting from apomorphine-induced degeneration on the dopaminergic system and the efficacy of treatment were evaluated in rats created as a model of PD. The average values and standard deviations of the number of rotations performed in this test are shown in Fig. 5A. According to this figure, 14 days after treatment, a significant result was obtained in the average number of rotations in the 6-OHDA group (212.5 rotation) compared to the control group and in the 6-OHDA + ZnNP + L-Dopa 60 group compared to the 6-OHDA group (87.5 rotation) ($p < 0.05$). In short, while the number of rotations increased in the 6-OHDA group, a significant decrease was observed in the treatment groups, dose-dependently, especially in the 6-OHDA + ZnNP + L-Dopa group. These data demonstrated the protective effect of L-Dopa-modified ZnNP treatment on striatal dopaminergic neurons.

The total distance traveled by the rats in the locomotor activity test is shown in Fig. 5B. Our research results demonstrated that the combination therapy had a neuroprotective effect on 6-OHDA-induced nigrostriatal injury in the locomotor rat model. According to these results, the total distance traveled was found to be significant in the 6-OHDA group (1013.69 cm) compared to the control group and in the 6-OHDA + L-Dopa 20 (1258.63 cm), 6-OHDA + ZnNP 20–40 (1276.09 and 1280.25 cm), and 6-OHDA + ZnNP + L-Dopa 60 (1425.52 cm) groups compared to the control group ($p < 0.05$). In short, while walking distance decreased in the 6-OHDA group, it increased significantly in the treatment groups, dose-dependently, especially in the 6-OHDA + ZnNP + L-Dopa group.

The effect of anxiety level on behavior in the elevated plus maze test is shown in Fig. 5C. According to the results, 6-OHDA was significant compared to the control group, 6-OHDA + L-Dopa 20 and 6-OHDA + ZnNP + L-Dopa 30–60 groups ($p < 0.05$). 6-OHDA increased the time spent compared to the control group, suggesting an anxiogenic-like behavior. Furthermore, the effect of 6-OHDA was reversed when mice were treated with their combination. Meanwhile, the combined treatment had a greater effect on Parkinson's mice than the treatments alone.

Selections related to the use of the forelimbs in rats with the roller test are shown in Fig. 5D. In our study, the paw in which we expected a functional decrease was the left paw (contralateral to the lesioned side). In the results obtained, 6-OHDA was found to be significant in the use of the right paw and double paw compared to the control group, and the 6-OHDA + L-Dopa 20 and 6-OHDA + ZnNP + L-Dopa 30–60 groups were also found to be significant in the use of the right paw and double paw compared to the 6-OHDA group ($p < 0.05$).

This physical adsorption process involves the binding of NH_2 and COOH groups of L-Dopa to the ZnNP surface via non-covalent interactions. Due to the nature of these bonds, L-Dopa can be released from ZnNPs over time. L-Dopa is initially physically bound to ZnNPs but is released over time, thus ensuring its therapeutic efficacy sustainably. The physical adsorption of L-Dopa onto ZnNPs and its release over time supports the potential of these nanoparticles to be used as an effective drug delivery system³³.

Effects of L-Dopa-modified ZnNPs on EAAT-1, EAAT-2, GLUL, and PTEN gene expression

EAAT-1 gene expression was importantly downregulated in the 6-OHDA group compared to the control group ($p < 0.05$). The combination groups demonstrated an important dose-dependent rise in EAAT-1 gene expression compared to the 6-OHDA group ($p < 0.05$). There was no important distinct in EAAT-1 gene expression in the other treatment groups ($p > 0.05$) (Fig. 6A).

A downregulation of EAAT-2 gene expression was observed in the 6-OHDA group compared to the control group ($p < 0.05$). Treatment with the combination groups importantly up-regulated EAAT-2 gene expression

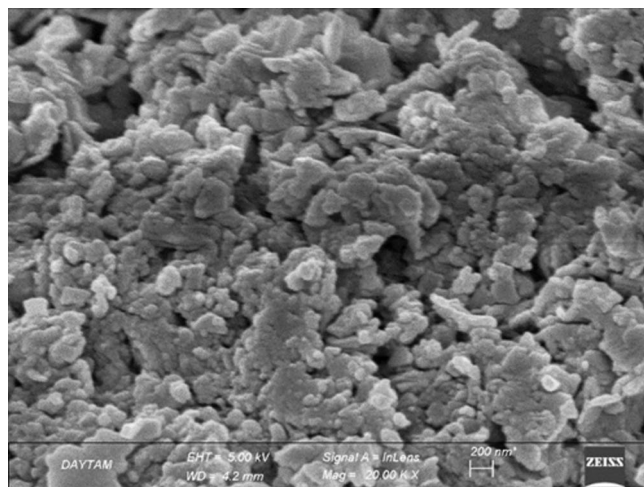


Figure 4. SEM images of ZnNPs.

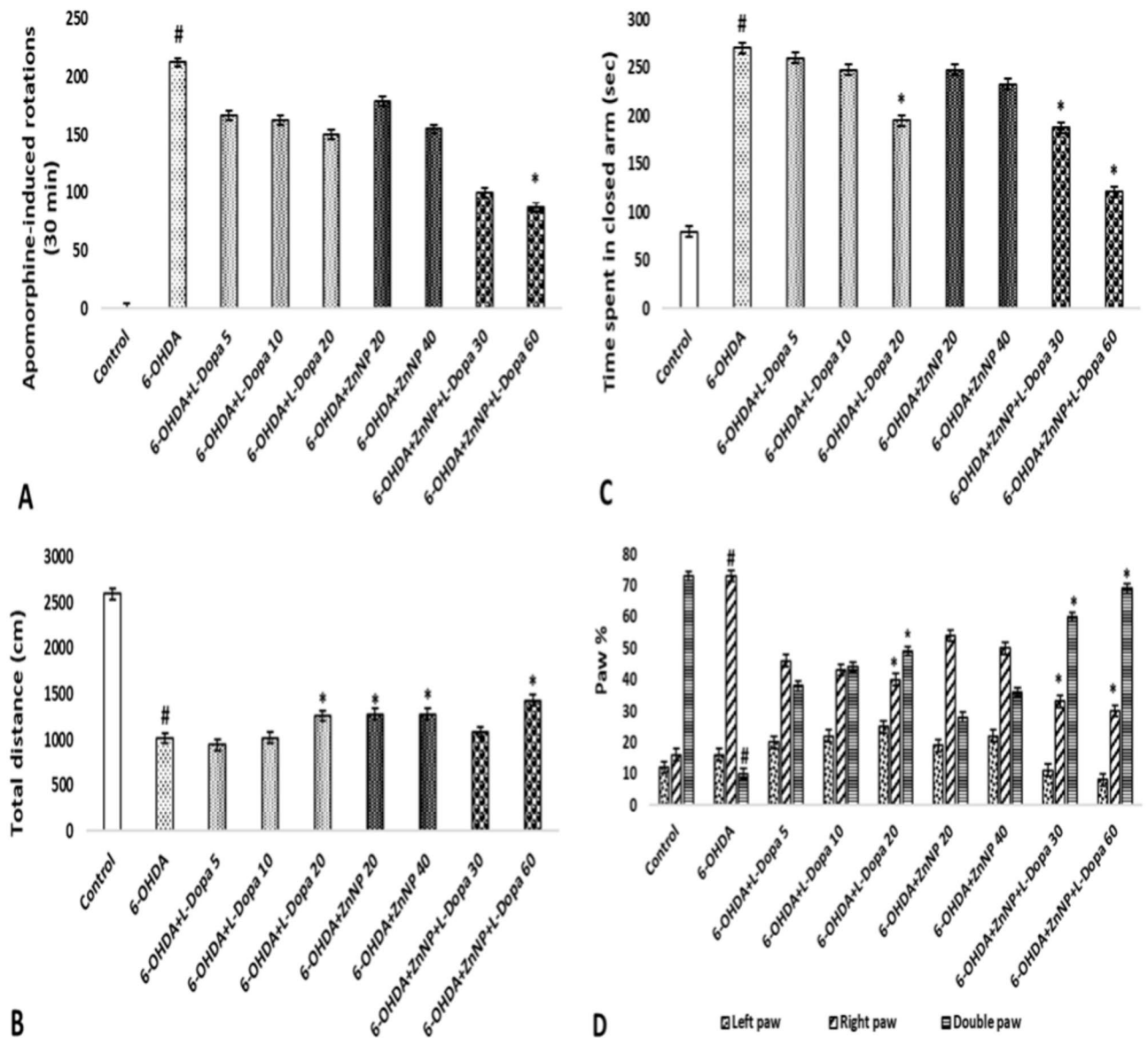


Figure 5. The effects of L-Dopa-modified ZnNPs on behavioral tests of PD rats. (A) Counterlateral rotation numbers. (B) Total length of distance travelled. (C) Time spent in the closed arm. (D) Forelimb usage percentages. # $p < 0.05$ compared to control and * $p < 0.05$ compared to 6-OHDA, (n = 8).

in a dosages-dependent way, nearly to the level of the control group. Furthermore, no significant difference in EAAT-2 gene expression was observed in the other treatment groups ($p > 0.05$) (Fig. 6B).

In the state of GLUL gene expression, we observed a significant down-regulation in the 6-OHDA group compared to the control group ($p < 0.05$). Therapy with the combination groups was able to significantly upregulate GLUL gene expression in a dosages-dependent way, nearly to the level of the control group ($p < 0.05$). No important distinct in GLUL gene expression was observed in the other therapy groups ($p > 0.05$) (Fig. 6C).

An important rise in PTEN gene expression was observed in the 6-OHDA group compared to the control group. Treatment with the combination groups was able to significantly upregulate PTEN gene expression in a dosages-dependent way, nearly to the level of the control group ($p < 0.05$). Furthermore, no important distinct in EAAT-2 gene expression was observed in the other treatment groups ($p > 0.05$) (Fig. 6D).

L-Dopa-modified ZnNPs prevent severe histopathological degeneration of brain tissue 6-OHDA-induced

Statistically important distinct were found between the groups in histopathological evaluation (Fig. 7, $p < 0.05$).

No important histopathological changes were found in the substantia nigra of rats in the control group. Severe pyknotic neurons were observed in the 6-OHDA and 6-OHDA + L-Dopa 20 groups, whereas moderate pyknotic neurons were observed in the 6-OHDA + L-Dopa 5, 6-OHDA + L-Dopa 10 and 6-OHDA + ZnNP + L-Dopa 60 groups. In the 6-OHDA + ZnNP 20, 6-OHDA + ZnNP 40, and 6-OHDA + ZnNP + L-Dopa 30 groups, this level

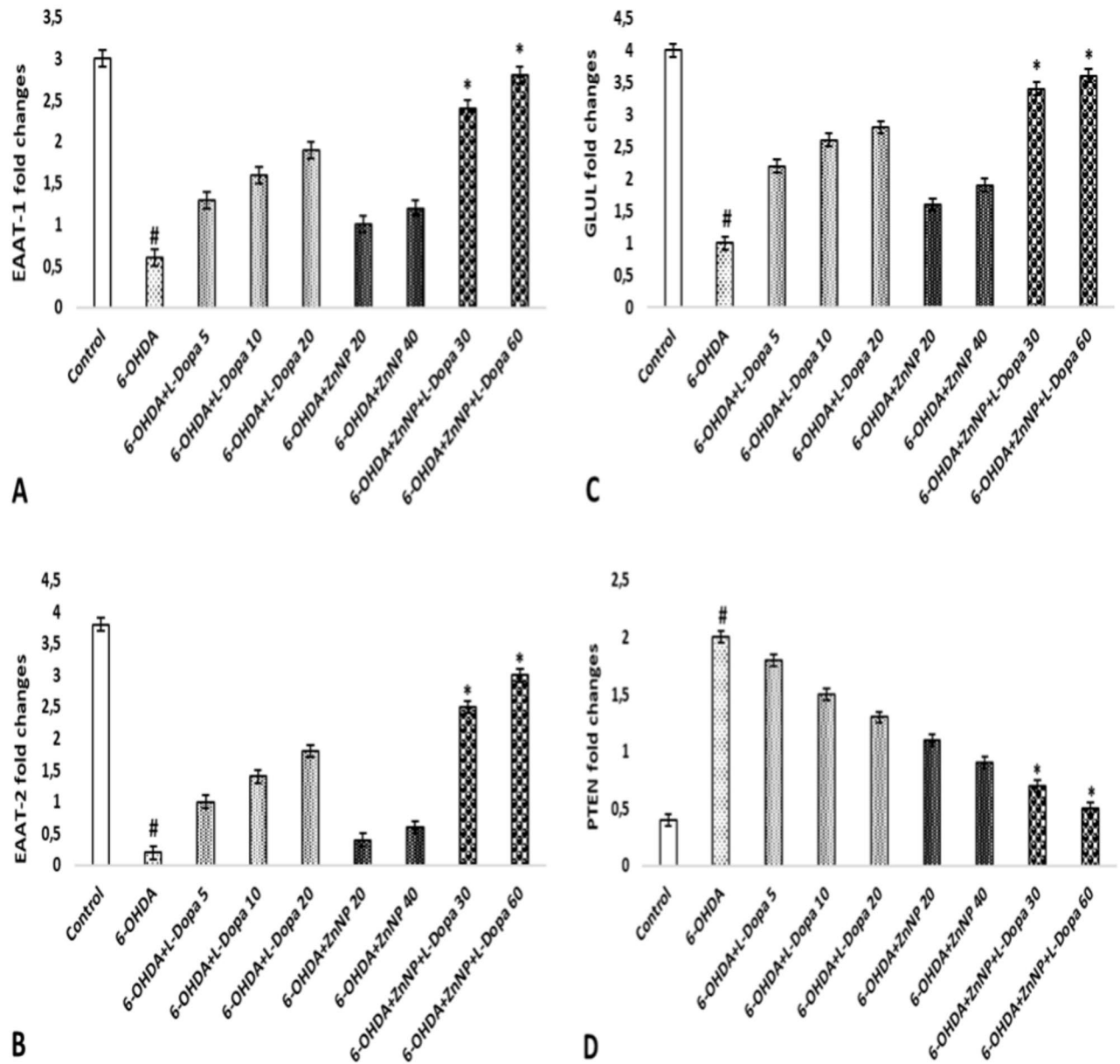


Figure 6. EAAT1, EAAT2, GLUL, and PTEN gene expression. (A) EAAT1. (B) EAAT2, (C) GLUL, (D) PTEN. # $p < 0.05$ compared to control and * $p < 0.05$ compared to 6-OHDA, ($n = 4$).

of pyknotic neurons was mild pyknotic neurons was mild. Glial cell activation was parallel to the severity of pyknotic neurons. In groups where pyknotic neurons were severe, moderate, and mild, glial cell activation was similarly severe, moderate, and mild, respectively (Figs. 8, 9).

To distinguish between direct effects on neuronal cells and potential indirect effects mediated by immune cells, we are incorporating advanced imaging techniques and histological analyses. This will help us determine whether the nanoparticles exert a direct influence on brain cells or if their effects are mediated through interactions with monocytes or macrophages. It is seen in Fig. 8 that the findings obtained from L-Dopa-modified ZnNPs penetrate the brain.

Effects of L-Dopa-modified ZnNPs on α -synuclein and GFAP levels in brain tissue

Immunohistochemical staining of SN for α -synuclein and GFAP revealed statistically important distinctions between the groups (Fig. 10, $p < 0.05$).

Immunohistochemical staining for α -synuclein showed no significant immunopositivity in the control group. While strong immunopositivity was observed in the 6-OHDA, 6-OHDA + L-Dopa 20, and 6-OHDA + ZnNP + L-Dopa 60 groups, moderate immunopositivity was observed in the 6-OHDA + L-Dopa 5 and 6-OHDA + L-Dopa 10 groups. Mild α -synuclein immunopositivity was seen in the 6-OHDA + ZnNP 20, 6-OHDA + ZnNP 40, and 6-OHDA + ZnNP + L-Dopa 30 groups (Figs. 11, 12).

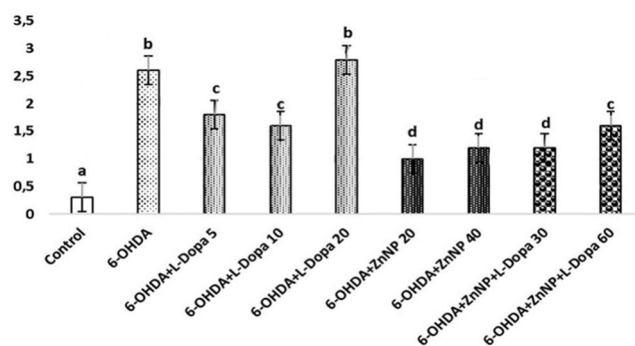


Figure 7. Pyknosis in neurons, and glial cell activation. (a–d) Show the difference between groups, $p < 0.05$). (a) Control group versus other groups, (b) 6-OHDA and 6-OHDA + L-Dopa 20 groups versus other groups, (c) 6-OHDA + L-Dopa 5, 6-OHDA + L-Dopa 10 and 6-OHDA + ZnNP + L-Dopa 60 groups versus other groups, (d) 6-OHDA + ZnNP 20, 6-OHDA + ZnNP 40 and 6-OHDA + ZnNP + L-Dopa 30 groups versus other groups, (n = 4).

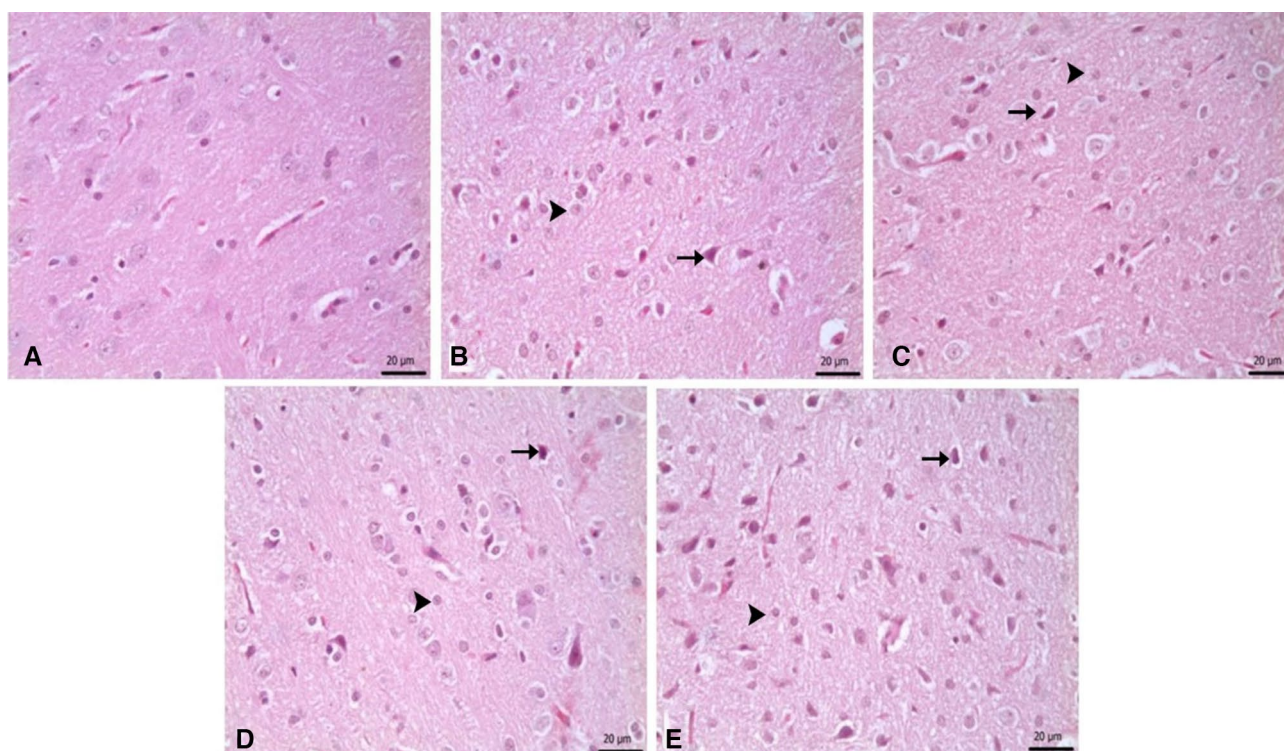


Figure 8. (A) Control group. Normal histological appearance. (B) 6-OHDA group. Severe level in pyknotic neurons, and glial cells, (C) L-Dopa 5 group. Medium level in pyknotic neurons, and glial cells, (D) L-Dopa 10 group. Medium level in pyknotic neurons, and glial cells, (E) L-Dopa 20 group. Severe level pyknotic changes in pyknotic neurons (arrows), and glial cells (arrowheads), H-E.

In immunohistochemical staining for GFAP, immunopositivity was less than that for α -synuclein. In the 6-OHDA, 6-OHDA + L-Dopa 5, and 6-OHDA + L-Dopa 10 groups, a low level of positivity was detected in SN neutrophils, whereas no significant positivity was detected in the other groups (Figs. 13, 14).

Discussion

Dyshomeostasis of Zn ions has been reported in many neurodegenerative and psychiatric disorders, including PD. Thus, altering brain Zn levels is a novel goal for avoiding and treating neurological and psychiatric disorders. L-Dopa remains the standard of care for the symptomatic treatment of PD and slowing disease progression; however, induction of oxidative stress in cells also leads to cell death by apoptosis³⁴. Currently, the synthesis of nano delivery systems containing L-Dopa is increasing to reduce the risk of dyskinesia, motor fluctuations, and other related side effects that develop as a result of long-term treatment with L-Dopa^{35,36}. In this study, we

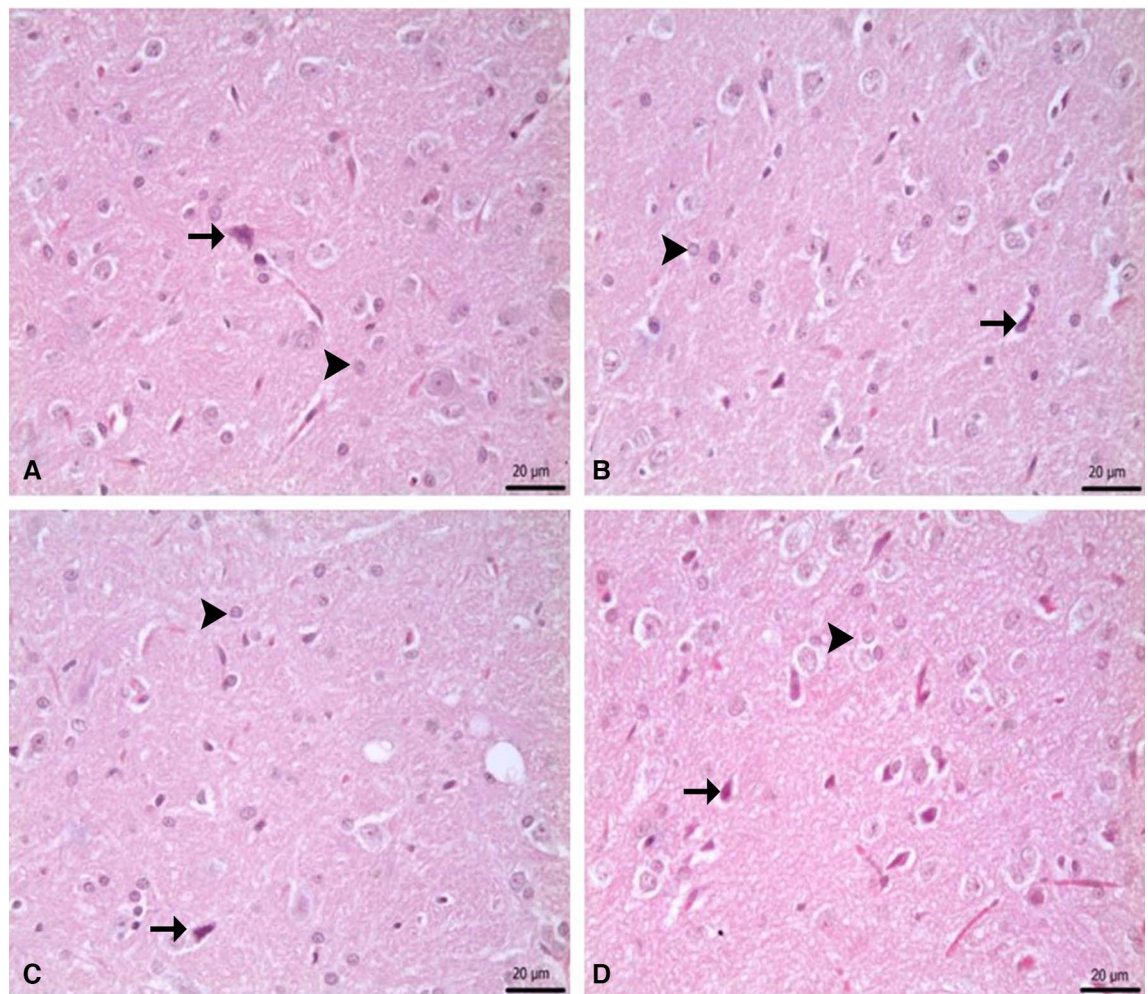


Figure 9. (A) 6-OHDA + ZnNP 20 group. (B) 6-OHDA + ZnNP 40 group. (C) 6-OHDA + ZnNP + L-Dopa 30 group. Mild level in pyknotic neurons, and glial cells, (D) 6-OHDA + ZnNP + L-Dopa 60 group. Moderate level pyknotic changes in pyknotic neurons (arrows), and glial cells (arrowheads), H-E.

researched the efficacy of L-Dopa-modified ZnNPs at distinct dosages in improving neurobehavioural and molecular parameters in oxidative stress-induced cytotoxicity induced by intrastriatal 6-OHDA injection.

The circular frequency of rats with PD is a major marker of damage to dopaminergic neurons in the SN²⁰. Administration of agonists such as apomorphine results in asymmetric behavior contralateral to the injured site. Therefore, unilateral 6-OHDA stereotaxic induction can be confirmed by measuring the number of these rotations³⁷. In the current study, we showed that L-Dopa-modified ZnNPs could significantly improve the brain functions of rats, resulting in protective effects on dopaminergic neurons in the rat SN. The results demonstrated the variable efficacy of the dosages in improving motor dysfunction in behavioral tests compared to untreated rats. In our study, ZnNP + L-Dopa showed a protective effect against 6-OHDA-induced injury to striatal neurons in an empirical model of PD. Treatment with 6-OHDA + ZnNP + L-Dopa reduced apomorphine-induced contralateral rotary movements at both doses. In the present study, 6-OHDA caused an important corruption of bradykinesia, motor skills, coordination, and loss of stability. The motor impairment may be described by striatal dopamine depletion, which has been previously reported in PD³⁸. The current data demonstrated that striatal dopamine was importantly reduced by 6-OHDA injection, supplying proof to promote this model.

The difference between the cylinder test and the apomorphine-induced rotational test is that no chemical agents are used to evaluate the developing motor asymmetry and it allows for a more sensitive evaluation in measuring dopamine denervation³⁹. In our study, the groups' percentage of using the front paw was evaluated. Claw use decreased in the 6-OHDA group compared to the control group. The motor asymmetry observed due to 6-OHDA toxicity is an expected finding and shows that the PD has been successfully implemented. This result is compatible with previous data^{39,40}. Ipsilateral paw use as a result of 6-OHDA neurotoxin in the sensorimotor cortex may cause motor asymmetry by causing deficits in sensorimotor and somatosensory functions^{25,40}. This indicates that the dopamine level in the nigrostriatal pathway decreases and the ipsilateral paw is used at the maximum level²⁵. It is seen that the ipsilateral paw percentage of the L-Dopa-modified ZnNP groups approaches the control group value. These data suggest that the use of ZnNP alone is not as effective as L-Dopa in correcting

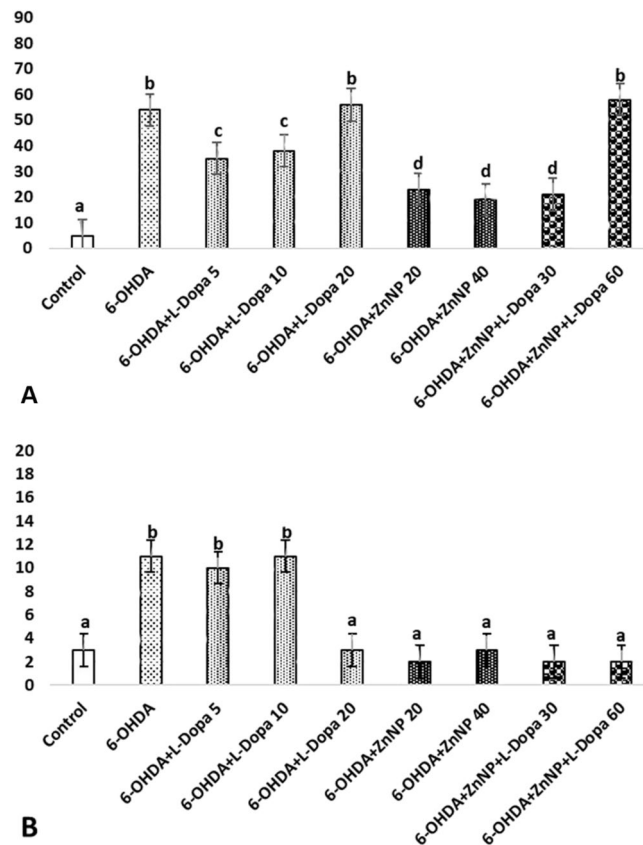


Figure 10. (a–d) Show the difference between groups, $p < 0.05$. (A) α -synuclein immunopositivity, (a) control group versus other groups, (b) 6-OHDA, 6-OHDA + L-Dopa 20 and 6-OHDA + ZnNP + L-Dopa 60 groups versus other groups, (c) 6-OHDA + L-Dopa 5 and 6-OHDA + L-Dopa 10 groups versus other groups, (d) 6-OHDA + ZnNP 20, 6-OHDA + ZnNP 40 and 6-OHDA + ZnNP + L-Dopa 30 groups versus other groups. (B) GFAP expressions immunopositivity, (a) control, 6-OHDA + L-Dopa 20, 6-OHDA + ZnNP 20, 6-OHDA + ZnNP 40, 6-OHDA + ZnNP + L-Dopa 30 and 6-OHDA + ZnNP + L-Dopa 60 groups versus other groups, (b) 6-OHDA, 6-OHDA + L-Dopa 5 and 6-OHDA + L-Dopa 10 group versus other groups, ($n = 4$).

motor asymmetry, but the modification of ZnNP with L-Dopa provides an improvement in sensorimotor performance by increasing the effectiveness of L-Dopa and accordingly corrects motor asymmetry.

Activity meter tests allow us to obtain information about spontaneous locomotor and exploratory movements and motor damage in experimental animals. It has been reported that 6-OHDA applied to rats caused deterioration in locomotor activity due to the degeneration of neurons. While a decrease in dopamine concentration causes hypoactivity, an increase results in hyperactivity^{39,41}. In this study, the distance traveled was evaluated with the locomotor activity test. It was found that the distance traveled in the 6-OHDA group was reduced compared to the control group. Changing locomotor activity in the 6-OHDA group is an expected finding, and the relationship between spontaneous locomotor activity and dopaminergic degeneration has been shown in PD models^{41,42}. The distance traveled in the groups treated with L-Dopa-modified ZnNP was compared with the 6-OHDA group and it was observed that the distance traveled increased. This also showed us that it preserves locomotor performance, which is associated with a neuroprotective effect and preservation of endogenous dopamine levels. Elevated plus maze results also correlate with locomotor activity. Increasing drug doses has been shown to reduce closed-arm stays.

It is thought that the motor deficits seen in animal models of PD induced by experimental 6-OHDA are directly related to the dopaminergic system⁴¹. L-Dopa, known as a dopamine agent, shows its effectiveness in early treatment through dopaminergic transmission. In this study, early treatment with L-Dopa was preferred and it was observed that it provided significant improvement in the behavioral tests performed. This finding is consistent with the literature⁴⁰. When the ZnNP-treated group was compared with the L-Dopa-treated group, it was observed that the effect of ZnNP alone was not as therapeutic as L-Dopa. In addition, it was determined that ZnNP increased the effectiveness of L-Dopa in groups treated with L-Dopa-modified ZnNP. It is thought that ZnNP prolongs the effect duration of L-Dopa by increasing the motor functional connections of L-Dopa and thus contributes to the therapeutic efficiency of L-Dopa by maximizing the improvement in motor performance. The proposed description for such healing in motor activity is the restoration of striatal dopamine levels by L-Dopa-modified ZnNP treatment.

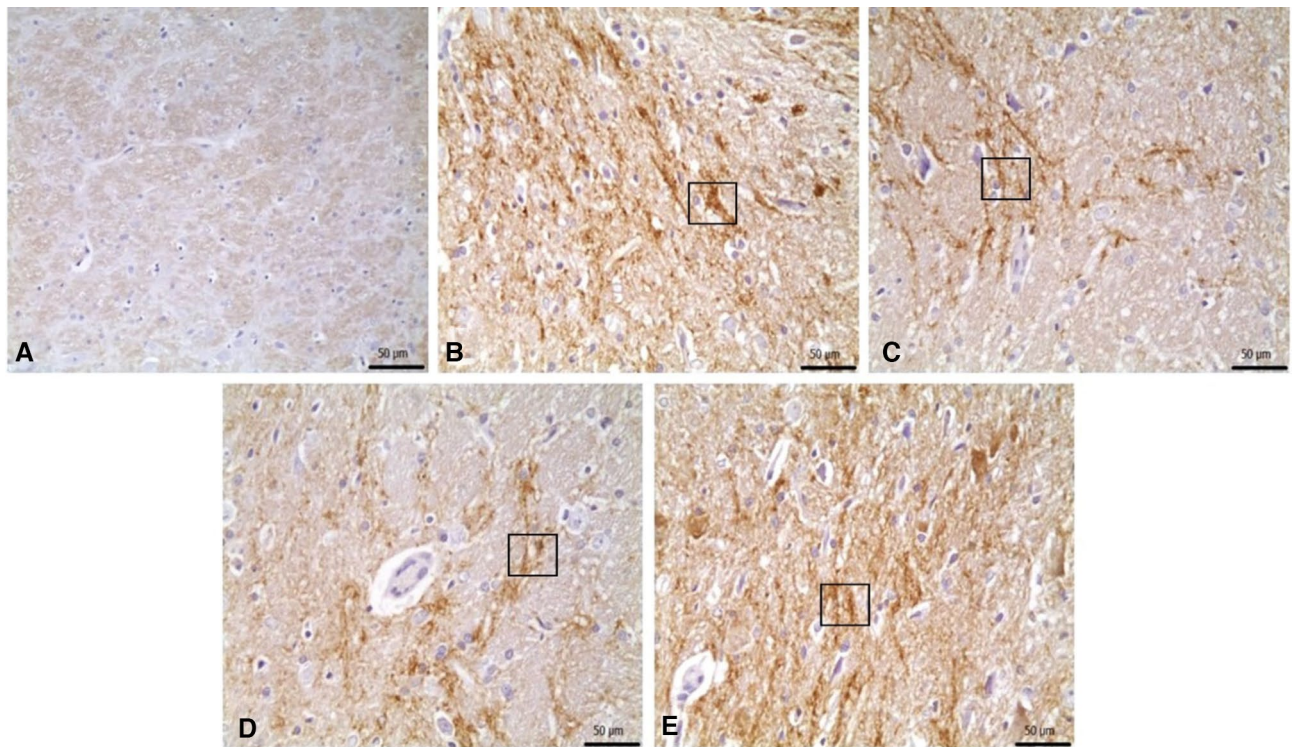


Figure 11. (A) Control group, a synuclein immunonegativity, (B) 6-OHDA group. Severe level, (C) L-Dopa 5 group. Moderate level, (D) L-Dopa 10 group. Moderate level, (E) L-Dopa 20 group. Severe level a synuclein immunopositivity (□), IHC.

Glutamate is one of the major neurotransmitters of the central nervous system and plays a significant role in various brain functions⁴³. However, it can also cause neurotoxicity. This occurs through excessive glutamatergic stimulation of glutamate receptors and can lead to the death of dopaminergic neurons, resulting in movement disorders and cognitive impairment⁴⁴. Previous studies have demonstrated that EAAT expression is decreased in PD patients and animal models^{45,46}. In our study, impaired glutamate uptake and decreased EAAT-1, EAAT-2, and GLUL expression were observed in the 6-OHDA-induced PD model. As EAAT-2 is mainly responsible for glutamate uptake, there is increasing evidence suggesting a role for EAAT-2 in PD^{45,47}. The use of an EAAT-2 inhibitor blocks glutamate reuptake and reduces dopamine synthesis⁴⁷. These findings suggest that EAAT-2 dysfunction plays a role in the progression of PD. However, a study in which the glutamate transporter L-trans-pyrrolidine-2,4-dicarboxylate inhibitor was injected into the unilateral substantia nigra of rats reported dopamine neuron death and axon dystrophy. It was shown that the cause of motor impairment in rats was related to the loss of dopamine neurons⁴⁸. Furthermore, this study provides solid evidence for the association of reduced glutamate transporter function with PD. We also observed increased expression of PTEN, which is important in neurodevelopment. In particular, L-Dopa-modified ZnNPs decreased PTEN expression in a dose-dependent way, as PTEN regulates both the density and strength of glutamatergic synapses. Accordingly, overexpression of PTEN, one of the dominant determinants of neuronal cell death, has become a potency molecular goal for novel therapeutic strategies against PD^{49,50}.

Histological findings support molecular and behavioral findings. Histological examination of rats receiving 6-OHDA showed that 6-OHDA contributed to some histological changes in neurons in the SN regions. On the other hand, increased oxidative stress caused by 6-OHDA was associated with neuronal damage in the SN. In our study, 6-OHDA was shown to cause pyknotic changes in SN neurons. In support of our findings, studies have reported neuronal cell death in 6-OHDA lesioned animals^{51,52}. Our results show that L-Dopa modified ZnNP application can ameliorate the damage to neurons in the SN. In addition, the 6-OHDA + L-Dopa groups had little effect on the repair of damaged tissue. Histopathological changes were mild in ZnNP-treated rats. These results confirmed that ZnNPs have no toxic effect on brain tissue⁵³. Gantedi et al. 5 mg/kg ZnNP did not reason any important alterations in the brain histology of rats one month after treatment⁵⁴. Our results are in deal with these studies.

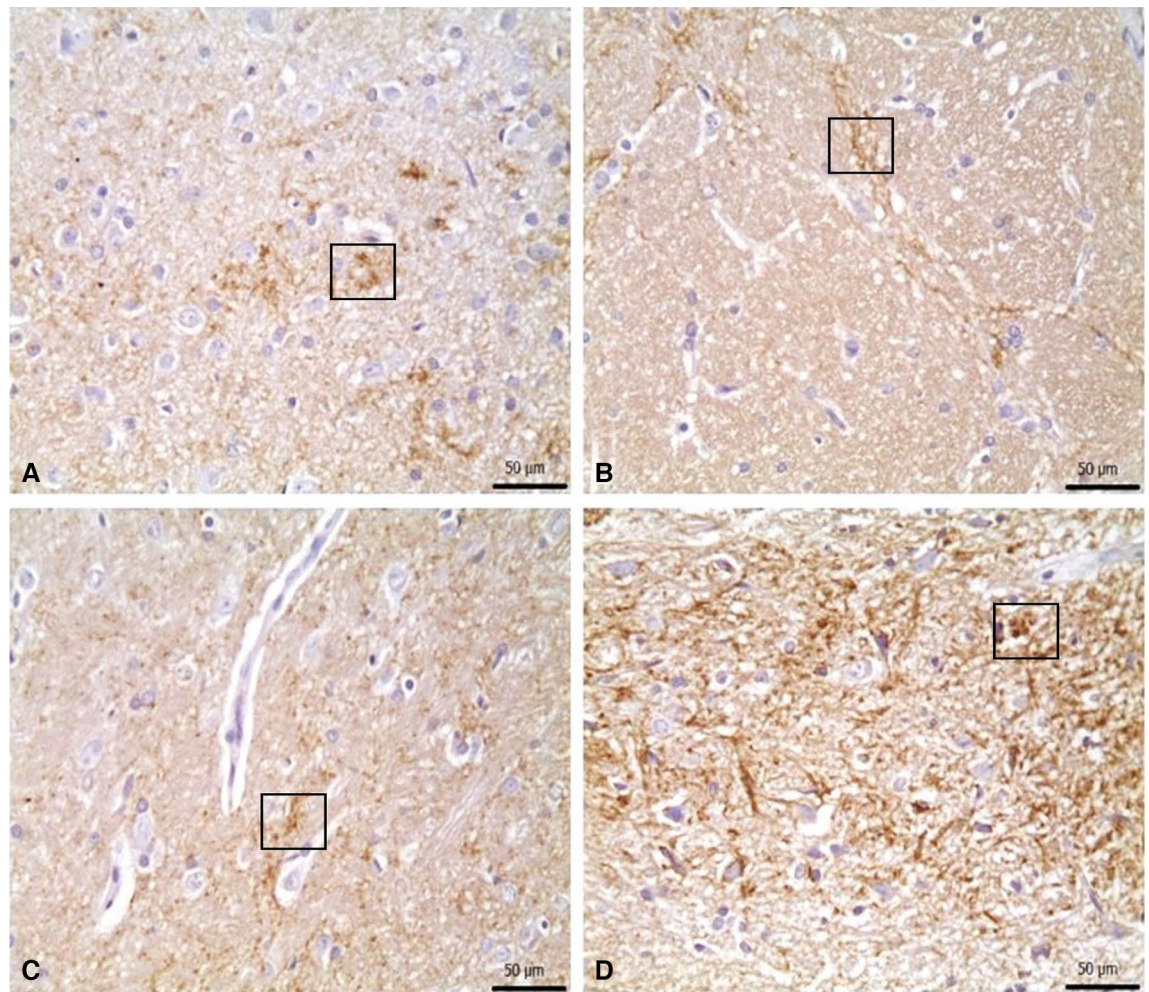


Figure 12. (A) 6-OHDA + ZnNP 20 group, (B) 6-OHDA + ZnNP 40 group, (C) 6-OHDA + ZnNP + L-Dopa 30 group. Mild level, (D) 6-OHDA + ZnNP + L-Dopa 60 group. Severe level α synuclein immunopositivity (\square), IHC.

α -Synuclein is primarily found in neurons, but usually after diffusing from neurons^{55,56}, it can also accumulate in astrocytes, via cell-to-cell transfer⁵⁷. Moreover, in neurodegenerative conditions such as PD, intracellular accumulation of α -synuclein occurs⁵⁸. There is ample evidence showing that α -synuclein overexpression increases oxidative stress levels^{59,60}. It has been shown that the level of α -synuclein increases in the rat model of PD accompanied by 6-OHDA-induced autophagy impairment⁶¹, a situation also observed in our study. In the presence of L-Dopa-modified ZnNPs, the increase in α -synuclein level decreases. Additionally, there were higher GFAP levels in the group with 6-OHDA lesions in the SN; this showed the development of astrocytosis and inflammation in the nigrostriatal system, consistent with previous reports⁶². ZnNP and L-Dopa-modified ZnNPs were able to reduce GFAP overexpression in striatal lysate, which may be due to its anti-inflammatory properties. Briefly, our results show that L-Dopa-modified ZnNP reverses 6-OHDA-induced damage and promotes tissue regeneration.

Conclusion

Considering the doses and properties of L-Dopa-modified ZnNPs studied, it was shown that L-Dopa-modified ZnNPs exerted an ameliorative effect against 6-OHDA by reducing oxidative stress and raising the expression levels of glutamate transporters, resulting in repair of tissue abnormalities and improvement of motor activities. This finding suggests that it may attenuate the progression of PD by suppressing 6-OHDA-mediated damage. It also supports the potential therapeutic applications of L-Dopa-modified ZnNPs as an adjunct in the therapy of PD. On the other hand, further studies are needed before the ultimate role of nanoparticles can be applied in the medical field.

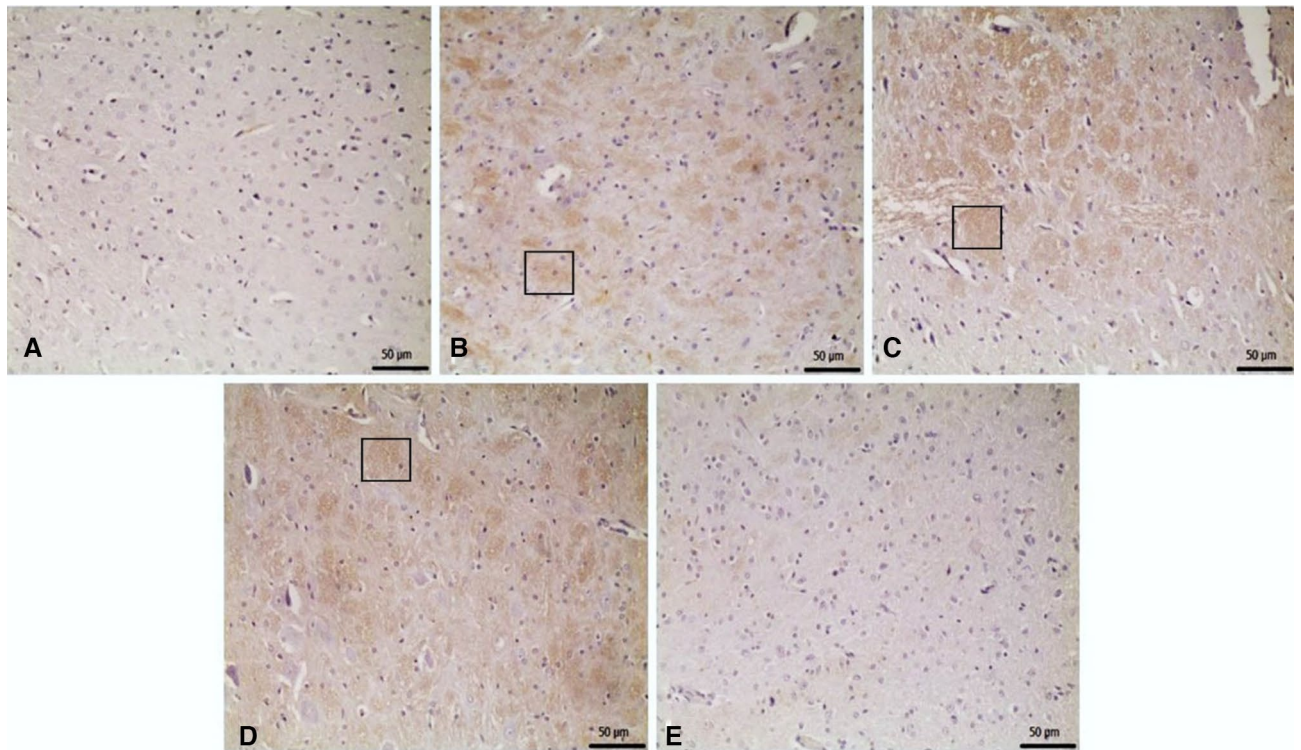


Figure 13. (A) Control group, GFAP immunopositivity, (B) 6-OHDA group, (C) L-Dopa 5 group, (D) L-Dopa 10 group. Mild level GFAP immunopositivity (□), (E) L-Dopa 20 group. GFAP immunonegativity, IHC.

Although the current study shows that L-Dopa-modified ZnNPs have neuroprotective properties and have the potential to increase dopamine levels in PD, they have certain limitations that should be noted. Firstly, our study was conducted on an animal model, further research is necessary to determine the safety and effectiveness of the treatment in humans. Neurobehavior, molecular, histopathological, and Immunohistochemical analysis were the main topics of our research. However, PD also involves various markers, including proinflammation, oxidative stress, and mitochondrial dysfunction. The broader impact of L-Dopa-modified ZnNP therapies on these factors should be investigated. The short study duration may have led to overlooking the potential long-term effects of L-Dopa-modified ZnNP therapies. These limitations highlight the need for further research to fill these knowledge gaps and provide a comprehensive understanding of the therapeutic potential of NPs for PD.

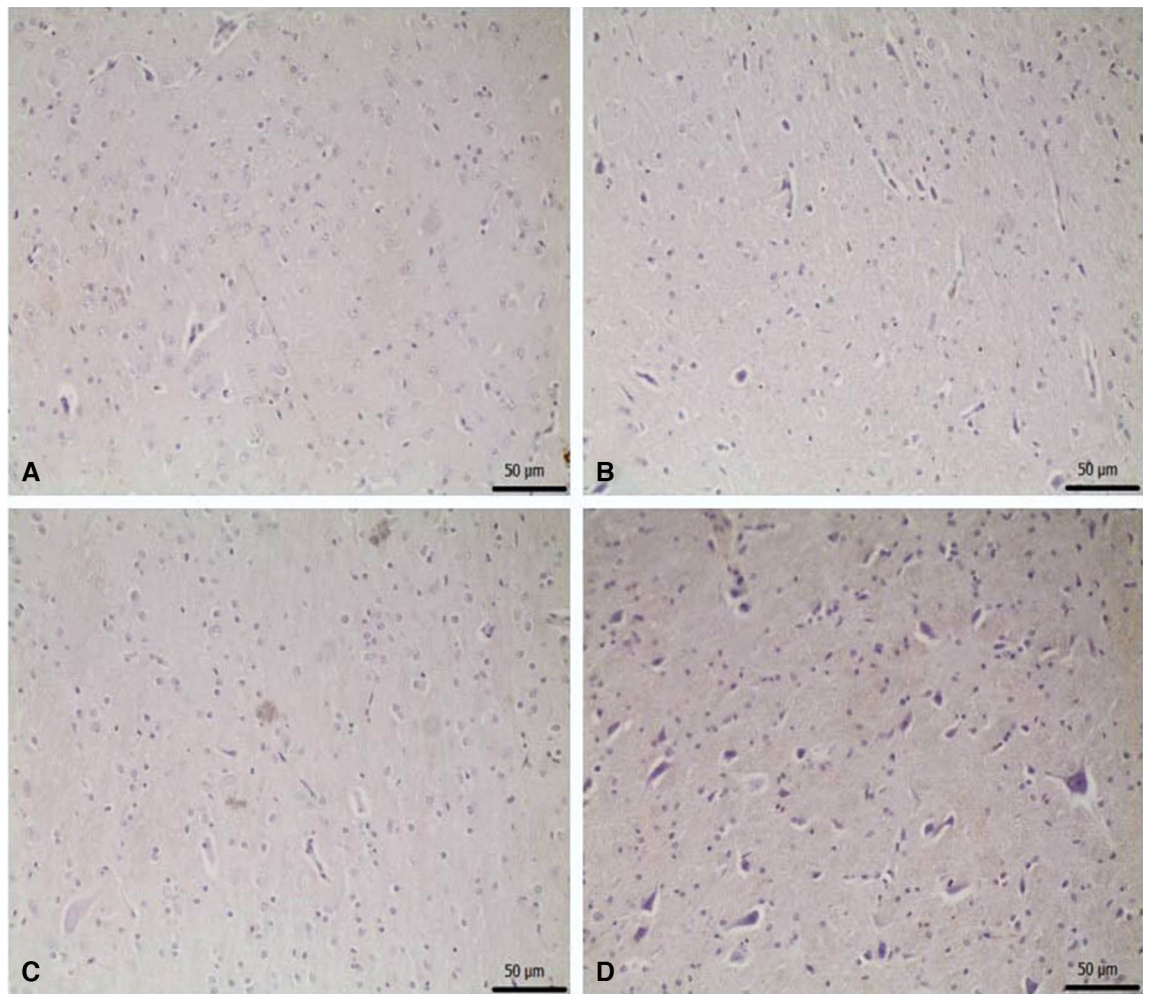


Figure 14. (A) 6-OHDA + ZnNP 20 group, (B) 6-OHDA + ZnNP 40 group, (C) 6-OHDA + ZnNP + L-Dopa 30 group, (D) 6-OHDA + ZnNP + L-Dopa 60 group. GFAP immunonegativity, IHC.

Data availability

Data is provided within the manuscript or supplementary information files. The datasets used and/or analysed during the current study available from the corresponding author on reasonable request.

Received: 17 April 2024; Accepted: 2 August 2024

Published online: 17 August 2024

References

- Pollanen, M. S., Dickson, D. W. & Bergeron, C. Pathology and biology of the Lewy body. *J. Neuropathol. Exp. Neurol.* **52**(3), 183–191 (1993).
- Carlsson, T., Bjorklund, T. & Kirik, D. Restoration of the striatal dopamine synthesis for Parkinson's disease: Viral vectormediated enzyme replacement strategy. *Curr. Gene Ther.* **7**, 109–120 (2007).
- Salawu, F. K., Danburam, A. & Olokoba, A. B. Non-motor symptoms of Parkinson's disease: Diagnosis and management. *Niger. J. Med.* **19**(2), 126–131 (2010).
- Sveinbjornsdottir, S. The clinical symptoms of Parkinson's disease. *J. Neurochem.* **139**, 318–324 (2016).
- Leyva-Gómez, G. *et al.* Nanoparticle technology for treatment of Parkinson's disease: The role of surface phenomena in reaching the brain. *Drug Discov. Today* **20**, 824–837 (2015).
- Aquino, C. C. & Fox, S. H. Clinical spectrum of levodopa-induced complications. *Mov. Disord.* **30**(1), 80–89 (2015).
- García-Moreno, J. M., Páramo, L. & Chacon, J. Oral L-dopa solution therapy of menstrual-related fluctuations in Parkinson's disease. *Parkinsonism Relat. Disord.* **10**, 53–54 (2003).
- Connolly, B. S. & Lang, A. E. Pharmacological treatment of Parkinson disease: A review. *JAMA* **311**(16), 1670–1683 (2014).
- Bisaglia, M., Filograna, R., Beltramini, M. & Bubacco, L. Are dopamine derivatives implicated in the pathogenesis of Parkinson's disease? *Ageing Res. Rev.* **13**, 107–114 (2014).
- Goldstein, D. S., Kopina, J. & Sharabi, Y. Catecholamine autotoxicity. Implications for pharmacology and therapeutics of Parkinson disease and related disorders. *Pharmacol. Ther.* **144**, 268–282 (2014).
- Ross, K. A. *et al.* Nano-enabled delivery of diverse payloads across complex biological barriers. *J. Control Release* **219**, 548–559 (2015).
- Richard, P. U. *et al.* New concepts to fight oxidative stress: Nanosized three-dimensional supramolecular antioxidant assemblies. *Expert. Opin. Drug Deliv.* **12**, 1527–1545 (2015).

13. Sandhir, R., Yadav, A., Sunkaria, A. & Singhal, N. Nano-antioxidants: An emerging strategy for intervention against neurodegenerative conditions. *Neurochem. Int.* **89**, 209–226 (2015).
14. Marcianes, P. *et al.* Surface-modified gatifloxacin nanoparticles with potential for treating central nervous system tuberculosis. *Int. J. Nanomed.* **12**, 1959–1968 (2017).
15. Chenthamara, D. *et al.* Therapeutic efficacy of nanoparticles and routes of administration. *Biomater. Res.* **23**, 20 (2019).
16. Xu, Q., Kambhampati, S. P. & Kannan, R. M. Nanotechnology approaches for ocular drug delivery. *Middle East Afr. J. Ophthalmol.* **20**(1), 26–37 (2013).
17. Nie, T. *et al.* Non-invasive delivery of levodopa-loaded nanoparticles to the brain via lymphatic vasculature to enhance treatment of Parkinson's disease. *Nano Res.* **14**(8), 2749–2761 (2021).
18. Khedr, M. *et al.* Neurobehavioural effect of zinc oxide nanoparticles and its conventional form on adult male rats and their pups. *Alex. J. Vet. Sci.* **66**, 36 (2020).
19. Nascimento, G. C. *et al.* Dynamic involvement of striatal NG2-glia in L-DOPA induced dyskinesia in Parkinsonian rats: Effects of doxycycline. *ASN Neuro* **15**, 17590914231155976 (2023).
20. Abdulmalek, S., Nasef, M., Awad, D. & Balbaa, M. Protective effect of natural antioxidant, curcumin nanoparticles, and zinc oxide nanoparticles against type 2 diabetes-promoted hippocampal neurotoxicity in rats. *Pharmaceutics* **13**(11), 1937 (2021).
21. Paxinos, G. & Watson, C. *The Rat Brain in Stereotaxic Coordinates: Hard Cover Edition* (Elsevier, 2006).
22. Ungerstedt, U. Postsynaptic supersensitivity after 6-hydroxy-dopamine induced degeneration of the nigro-striatal dopamine system. *Acta Physiol. Scand. Suppl.* **367**, 69–93 (1971).
23. Jin, F. *et al.* Neuroprotective effect of resveratrol on 6-OHDA-induced Parkinson's disease in rats. *Eur. J. Pharmacol.* **600**(1–3), 78–82 (2008).
24. Yeni, Y. *et al.* A selective histamine H4 receptor antagonist, JNJ777120, role on glutamate transporter activity in chronic depression. *J. Pers. Med.* **12**(2), 246 (2022).
25. Glajch, K. E., Fleming, S. M., Surmeier, D. J. & Osten, P. Sensorimotor assessment of the unilateral 6-hydroxydopamine mouse model of Parkinson's disease. *Behav. Brain Res.* **230**, 309–316 (2012).
26. Hamadjida, A., Frouni, L., Kwan, C. & Huot, P. Classic animal models of Parkinson's disease: A historical perspective. *Behav. Pharmacol.* **30**, 291–310 (2019).
27. Livak, K. J. & Schmittgen, T. D. Analysis of relative gene expression data using real-time quantitative PCR and the 2(T)–(Delta Delta C) method. *Methods* **25**, 402–408 (2001).
28. Arefi, M. R. & Rezaei-Zarchi, S. Synthesis of zinc oxide nanoparticles and their effect on the compressive strength and setting time of self-compacted concrete paste as cementitious composites. *Int. J. Mol. Sci.* **13**, 4340–4350 (2012).
29. Prasad, K. & Jha, K. A. ZnO nanoparticles: Synthesis and adsorption study. *Nat Sci.* **01**, 129–135 (2009).
30. Rajendran, S. P. & Sengodan, K. Synthesis and characterization of zinc oxide and iron oxide nanoparticles using sesbania grandiflora leaf extract as reducing agent. *J. Nanosci.* **2017**, 1–7 (2017).
31. Nalci, O. B. *et al.* Effects of ZnO, CuO and γ -Fe₃O₄ nanoparticles on mature embryo culture of wheat (*Triticum aestivum* L.). *Plant Cell Tissue Organ Cult.* **136**, 269–277 (2019).
32. Nadaroglu, H. & Alayli, A. Highly sensitive glucose sensor based on ZnO NPs as a biomimetic enzyme. *Biosci. Res.* **17**, 775–785 (2020).
33. Morales, V. *et al.* L-Dopa release from mesoporous silica nanoparticles engineered through the concept of drug-structure-directing agents for Parkinson's disease. *J. Mater. Chem. B* **9**(20), 4178–4189 (2021).
34. Parkkinen, L. *et al.* Does levodopa accelerate the pathologic process in Parkinson disease brain? *Neurology* **77**, 1420–1426 (2011).
35. Kura, A. U. *et al.* Development of a controlled-release anti-Parkinsonian nano delivery system using levodopa as the active agent. *Int. J. Nanomed.* **8**, 1103–1110 (2013).
36. Jaber, M. *et al.* Fate of L-DOPA in the presence of inorganic matrices: Vectorization or composite material formation? *J. Phys. Chem. C* **115**, 19216–19225 (2011).
37. Souza, R. B. *et al.* Neuroprotective effects of sulphated agaran from marine alga Gracilaria cornea in rat 6-hydroxydopamine Parkinson's disease model: Behavioural, neurochemical and transcriptional alterations. *Basic Clin. Pharmacol. Toxicol.* **120**, 159–170 (2017).
38. Richardson, J. R. & Hossain, M. M. Microglial ion channels as potential targets for neuroprotection in Parkinson's disease. *Neural Plast.* **2013**, 587418 (2013).
39. Su, R. J. *et al.* Time-course behavioral features are correlated with Parkinson's disease-associated pathology in a 6-hydroxydopamine hemiparkinsonian rat model. *Mol. Med. Rep.* **17**, 3356–3363 (2018).
40. de Araujo, D. P. *et al.* Behavioral and neurochemical effects of alpha-lipoic Acid in the model of Parkinson's disease induced by unilateral stereotaxic injection of 6-OHDA in rat. *Evid. Based Complement Alternat. Med.* **43**, 21–34 (2013).
41. Lima, L. A. *et al.* Vitamin D protects dopaminergic neurons against neuroinflammation and oxidative stress in hemiparkinsonian rats. *J. Neuroinflamm.* **15**, 1–11 (2018).
42. Singh, S. & Kumar, P. Piperine in combination with quercetin halt 6-OHDA induced neurodegeneration in experimental rats: Biochemical and neurochemical evidences. *Neurosci. Res.* **133**, 38–47 (2018).
43. Ferraguti, F., Crepaldi, L. & Nicoletti, F. Metabotropic glutamate 1 receptor: Current concepts and perspectives. *Pharmacol. Rev.* **60**, 536–581 (2008).
44. Sengul, G. *et al.* Neuroprotective effect of ACE inhibitors in glutamate-induced neurotoxicity: Rat neuron culture study. *Turk. Neurosurg.* **21**, 367–371 (2011).
45. Chung, E. K. Y., Chen, L. W., Chan, Y. S. & Yung, K. K. L. Downregulation of glial glutamate transporters after dopamine denervation in the striatum of 6-hydroxydopamine-lesioned rats. *J. Comp. Neurol.* **511**, 421–437 (2008).
46. Zhang, Y. L., Tan, F., Xu, P. Y. & Qu, S. G. Recent advance in the relationship between excitatory amino acid transporters and Parkinson's disease. *Neural Plast.* **2016**, 8941327 (2016).
47. Salvatore, M. F., Davis, R. W., Arnold, J. C. & Chotibut, T. Transient striatal GLT-1 blockade increases EAAC1 expression, glutamate reuptake, and decreases tyrosine hydroxylase phosphorylation at ser (19). *Exp. Neurol.* **234**, 428–436 (2012).
48. Assous, M. *et al.* Progressive Parkinsonism by acute dysfunction of excitatory amino acid transporters in the rat substantia nigra. *Neurobiol. Dis.* **65**, 69–81 (2014).
49. Gary, D. S. & Mattson, M. P. PTEN regulates Akt kinase activity in hippocampal neurons and increases their sensitivity to glutamate and apoptosis. *Nöromol. Med.* **2**, 261–269 (2002).
50. Kyrylenko, S., Roschier, M., Korhonen, P. & Salminen, A. Regulation of PTEN expression in neuronal apoptosis. *Brain Res. Mol. Brain Res.* **73**, 198–202 (1999).
51. Ghalami, J. *et al.* Paeonol protection against intrastriatal 6-hydroxydopamine rat model of Parkinson's disease. *Basic Clin. Neurosci.* **12**(1), 43–56 (2021).
52. Liu, Y.-Q. *et al.* Nanozyme scavenging ROS for prevention of pathologic α -synuclein transmission in Parkinson's disease. *Nano Today* **36**, 101027 (2021).
53. Hamza, R. Z., Al-Salmi, F. A. & El-Shenawy, N. S. Evaluation of the effects of the green nanoparticles zinc oxide on monosodium glutamate-induced toxicity in the brain of rats. *PeerJ* **23**(7), e7460 (2019).
54. Gantedi, S. & Anreddy, R. N. R. Toxicological studies of zinc oxide nanomaterials in rats. *Toxicol. Environ. Chem.* **94**(9), 1768–1779 (2012).

55. Braak, H., Sastre, M. & Del Tredici, K. Development of alpha-synuclein immunoreactive astrocytes in the forebrain parallels stages of intraneuronal pathology in sporadic Parkinson's disease. *Acta Neuropathol.* **114**(3), 231–241 (2007).
56. Fellner, L. & Stefanova, N. The role of glia in alpha-synucleinopathies. *Mol Neurobiol.* **47**(2), 575–586 (2013).
57. Angot, E. *et al.* Alpha-synuclein cell-to-cell transfer and seeding in grafted dopaminergic neurons in vivo. *PLoS ONE* **7**(6), e39465 (2012).
58. McCann, H., Stevens, C. H., Cartwright, H. & Halliday, G. M. a-Synucleinopathy phenotypes. *Parkinsonism Relat. Disord.* **20**, S62–S67 (2014).
59. Vali, S. *et al.* Insights into the effects of alpha-synuclein expression and proteasome inhibition on glutathione metabolism through a dynamic in silico model of Parkinson's disease: Validation by cell culture data. *Free Radic. Biol. Med.* **45**(9), 1290–1301 (2008).
60. Moon, H. E. & Paek, S. H. Mitochondrial dysfunction in Parkinson's disease. *Exp. Neurobiol.* **24**(2), 103–116 (2015).
61. Gu, X. S. *et al.* Neuroprotective effects of paeoniflorin on 6-OHDA-lesioned rat model of Parkinson's disease. *Neurochem. Res.* **41**, 2923–2936 (2016).
62. Calou, I. *et al.* Neuroprotective properties of a standardized extract from Myracrodruon urundeuva Fr. All. (Aroeira-Do-Sertao), as evaluated by a Parkinson's disease model in rats. *Parkinsons Dis.* **2014**, 519615 (2014).

Author contributions

Y.Y., Conceptualization (lead); data curation (equal); formal analysis (equal); writing—original draft (equal). S.G., Conceptualization (equal); data curation (equal); formal analysis (equal); writing—original draft (equal). M.S.E., Investigation (equal); formal analysis (equal); writing—original draft (equal). H.N.: Conceptualization (equal); investigation (equal); methodology (equal); writing—original draft (equal). A.G., Investigation (equal); methodology (equal); writing—original draft (equal). A.S.M., Formal analysis (equal); methodology (equal); writing—original draft (equal). A.H., Methodology (equal); writing—original draft (equal). Approval of the paper: all authors.

Funding

This research received no external funding.

Competing interests

The authors declare no competing interests.

Additional information

Correspondence and requests for materials should be addressed to Y.Y.

Reprints and permissions information is available at www.nature.com/reprints.

Publisher's note Springer Nature remains neutral with regard to jurisdictional claims in published maps and institutional affiliations.

Open Access This article is licensed under a Creative Commons Attribution-NonCommercial-NoDerivatives 4.0 International License, which permits any non-commercial use, sharing, distribution and reproduction in any medium or format, as long as you give appropriate credit to the original author(s) and the source, provide a link to the Creative Commons licence, and indicate if you modified the licensed material. You do not have permission under this licence to share adapted material derived from this article or parts of it. The images or other third party material in this article are included in the article's Creative Commons licence, unless indicated otherwise in a credit line to the material. If material is not included in the article's Creative Commons licence and your intended use is not permitted by statutory regulation or exceeds the permitted use, you will need to obtain permission directly from the copyright holder. To view a copy of this licence, visit <http://creativecommons.org/licenses/by-nc-nd/4.0/>.

© The Author(s) 2024